Journal of Nuclear Medicine, published on October 8, 2015 as doi:10.2967/jnumed.115.162024

Phase I study of ^{68}Ga-HER2-Nanobody for PET/CT assessment of HER2-expression in breast carcinoma

Marleen Keyaerts[1,2*], Catarina Xavier[2*], Johannes Heemskerk[1], Nick Devoogdt[2,3], Hendrik Everaert[1], Chloé Ackaert[3], Marian Vanhoeij[4], Francois P. Duhoux[5], Thierry Gevaert[6], Philippe Simon[7], Denis Schallier[8], Christel Fontaine[8], Ilse Vaneycken[1,2], Christian Vanhove[9], Jacques De Greve[8], Jan Lamote[4], Vicky Caveliers[1,2], Tony Lahoutte[1,2]

1. Nuclear Medicine Department, UZ Brussel, Brussels, Belgium.
2. In Vivo Cellular and Molecular Imaging Laboratory (ICMI), Vrije Universiteit Brussel, Brussels, Belgium.
3. Laboratory of Cellular and Molecular Immunology (CMIM), Vrije Universiteit Brussel, Brussels, Belgium.
4. Department of Oncological Surgery, UZ Brussel, Brussels, Belgium.
5. Medical Oncology, Cliniques universitaires Saint-Luc, Brussels, Belgium.
6. Department of Radiation Therapy, UZ Brussel, Brussels, Belgium.
7. Gynecology - Senology, Université Libre de Bruxelles - Hôpital Erasme, Brussels, Belgium.
8. Department of Medical Oncology, UZ Brussel, Brussels, Belgium.
9. iMinds Medical IT – IbiTech – Medisip - Infinity lab, Ghent University, Ghent, Belgium

* Contributed equally to this work.

Corresponding author: Marleen Keyaerts, Nuclear Medicine, UZ Brussel, Laarbeeklaan 101, 1090 Brussels, Belgium, +322-477-50-20, fax +322-477-50-17, marleen.keyaerts@vub.ac.be

Word count of manuscript: 5172

Financial support: MK and TL are Senior Clinical Investigators of the Research Foundation – Flanders (FWO). CV is supported by the GROUP-ID consortium of Ghent University. Research was funded by CancerPlan Action29 (Federal Public Service Health, Food Chain Safety and Environment, Belgium), Stichting tegen Kanker, FWO.

Running title: Phase I trial of ^{68}Ga-HER2-Nanobody PET/CT

Abstract

The HER2-status is one of the major tumor characteristics in breast cancer to guide therapy. Anti-HER2 treatment has clear survival advantages in HER2-positive breast carcinoma patients. Heterogeneity in HER2 expression has repeatedly been described between primary tumor and metastasis, resulting in the need to reassess HER2-status during the disease course. In order to avoid repeated biopsy with potential bias due to tumor heterogeneity, nanobodies directed against HER2 have been developed as probes for molecular imaging. Nanobodies are the smallest antigen-binding antibody fragments derived from unique heavy-chain-only antibodies, with ideal characteristics for positron emission tomography (PET) imaging. **Aim:** the primary aims were assessment of safety, biodistribution and dosimetry. The secondary aim was to investigate tumor targeting potential.

Methods: In total, 20 female patients with primary or metastatic breast carcinoma (HER2 IHC 2+ or 3+) were included. Anti-HER2-Nanobody is labeled with ^{68}Ga via a NOTA derivative. Administered activities were 53-174 MBq (average 107 MBq). PET/CT scans (for dosimetry assessment) were obtained at 10, 60 and 90 min post administration. Physical evaluation and blood analysis were performed for safety evaluation. Biodistribution was analyzed for 11 organs using MIM software; dosimetry was assessed using OLINDA/EXM. Tumor targeting potential was assessed in primary and metastatic lesions.

Results: No adverse reactions occurred. A fast blood clearance was observed, with only 10% of injected activity remaining in the blood at 1h post injection. Uptake was mainly seen in kidneys, liver, and intestines. The effective dose

was 0.043 mSv/MBq, resulting in an average of 4.6 mSv per patient. The critical organ was the urinary bladder wall with a dose of 0.406 mGy/MBq. In patients with metastatic disease, tracer accumulation well above background was demonstrated in the majority of identified sites of disease. Primary lesions were more variable in tracer accumulation.

Conclusion: ^{68}Ga-HER2-Nanobody PET/CT is a safe procedure with a radiation dose comparable to other routinely used PET tracers. Its biodistribution is favorable, with the highest uptake in kidneys, liver and intestines, but very low background levels in all other organs that typically house primary breast carcinoma or tumor metastasis. Tracer accumulation in HER2-positive metastases is high, compared to normal surrounding tissues, and warrants further assessment in a phase II trial.

Key words: Breast carcinoma, HER2, Nanobody, PET/CT, phase I.

Introduction

One in eight women develop breast cancer and it remains the second leading cause of cancer death in women. Identification of cancer subtypes, based upon biological markers, has led to the introduction of targeted therapies, with improved survival and morbidity. Besides hormone receptor expression, the Human Epidermal Growth factor receptor 2 (HER2) is used for breast cancer classification. Breast cancers with HER2 overexpression in primary and/or metastatic sites will benefit from HER2-targeted therapies such as the monoclonal antibody trastuzumab, resulting in a clear survival advantage (*1*).

Since only 20% of breast cancers overexpress HER2, the decision to start HER2-targeted therapy is based upon immunohistochemical assessment (IHC) or demonstrated gene amplification (e.g. Fluorescence in Situ Hybridization or FISH) on tumor tissue biopsy, usually obtained at initial diagnosis at the primary site. Only patients with strong expression of the protein (IHC 3+) or with strong amplification of the HER2 gene (FISH+) are selected for HER2-targeted therapy, as these patients gained the greatest clinical benefit from trastuzumab treatment (*1*). In the majority of therapeutic protocols, HER2-targeted therapy is given on top of a classical chemotherapy (e.g. paclitaxel, docetaxel). Recently, this approach has been optimized by linking a chemotoxin to the antibody, thereby specifically targeting it to HER2+ tumor cells. This compound, named trastuzumab-emtansine (T-DM1) showed improved efficacy while reducing toxicity (*2*).

Studies have shown HER2 testing discrepancy between local and large reference laboratories, resulting in 14-16% false-positive and 4% false-negative results (*3,4*). Such misclassification gives rise to unnecessary toxicity

and cost for the first, while denying a potentially efficacious therapy for the latter. Recently, several independent studies reported a significant discordance in HER2 expression between primary breast carcinoma and metastases ranging between 6% and 34%, as well as heterogeneity between metastases (*5-10*). Because of this discordance, the European guidelines now recommend to obtain a biopsy of a metastatic lesion, to reassess biological markers (*11*). With the increasing use of T-DM1, which only affects HER2-overexpressing cancer cells, the importance of correct HER2 assessment becomes even more important.

We here introduce the use of nanobodies directed against HER2 as probes for molecular imaging in breast carcinoma patients. Nanobodies are the smallest antigen-binding domains derived from unique heavy-chain-only antibodies that are naturally present in camelids. Nanobodies have proven to be ideal probes for SPECT- and PET- imaging in rodents, with high targeting potential and fast blood clearance (*12,13*). The anti-HER2-Nanobody 2Rs15d was selected and optimized as the lead compound for clinical translation (*14,15*). In this paper we report on the safety, biodistribution, dosimetry and tumor targeting potential of the ^{68}Ga-anti-HER2-Nanobody (^{68}Ga-HER2-Nanobody) in breast carcinoma patients.

Materials and Methods

Study design

This was an open-label phase I study in HER2-expressing breast carcinoma patients (n=20). The supplemental data provide details on patient selection and approvals. Three subgroups, receiving respectively 0.01 mg (group 1: pt 1–7),

0.1 mg (group 2: pt 8–15) and 1.0 mg (group 3: pt 16–20) NOTA-anti-HER2-Nanobody were evaluated. The activity administered was similar for the different patient groups and ranged between 53 and 174 MBq.

Imaging methods and safety assessment

Details on radioligand synthesis, safety assessment and PET/CT protocol are described in the supplemental data.

A *p*-SCN-Bn-NOTA chelator was conjugated to the Nanobody as described earlier (*15*). ^{68}Ga (250-400 MBq) was incubated with the NOTA-anti-HER2-Nanobody in acid conditions for 5-7 min at room temperature. ^{68}Ga-HER2-Nanobody was purified and filtered prior to injection. Quality controls included analysis of appearance, presence of ^{68}Ge, pH, radiochemical purity and radiochemical identity, filter integrity (bubble point test). For the different patient groups the necessary amount of cold NOTA-anti-HER2-Nanobody was added prior to final filtration.

^{68}Ga-HER2-Nanobody was injected as an intravenous bolus. For safety evaluation, vital sign were recorded and clinical laboratory testing was performed before and 2h after injection. Subjective adverse experiences were assessed using open questions up to 24h post injection (p.i.). Whole body PET/CT imaging (low-dose CT) was performed with a Philips Gemini TF at 10, 60 and 90 minutes p.i.

Summary blood, urine and image analysis

Details on image processing and analysis as well as blood and urine analysis and detection of anti-drug-antibodies (ADA) are described in the supplemental data.

Blood samples were obtained at different time points p.i., assessed for radioactive content and expressed as a percentage of the injected activity (%IA) in total blood volume using Nadler's formula. Urine samples were collected at about 45 min and 2h p.i. Blood and urine were assessed for metabolites.

Uptake in 11 organs (liver, kidneys, intestines, thyroid, whole body, bladder and urinary activity in ureters, spleen, heart muscle, lungs, hematopoietic bone marrow and breast tissue) was measured on each PET/CT using MIM contouring software (MIM-software Inc.) and expressed as %IA. Dosimetric calculations for the adult female were made using the OLINDA/EXM software 1.0 (*16*).

Uptake in tumor lesions was measured using the mean Standard Uptake Value (SUV_{mean}) in a 10 mm spheroid Region of interest (ROI) positioned over the area with the highest uptake. If available, the uptake in the primary lesion and in the metastasis showing the highest SUV_{mean} is reported.

Results

Patient Characteristics

Between April 2012 and July 2014, 20 patients completed the study protocol. The patients received on average 107 ± 37 MBq (range 53 - 174 MBq) ^{68}Ga-HER2-Nanobody. Patient and study drug characteristics are summarized in table 1.

Safety Assessment

After the administration of ^{68}Ga-HER2-Nanobody, no symptoms or signs were reported. Clinical laboratory testing of blood, taken before and 120 min after injection, showed no significant changes that could be related to the study drug. ADA were not detected in serum samples of 20 patients, taken before and 3 months after administration (Figure S1).

Pharmacokinetics and Biodistribution

Figure 1 shows images of representative patients for each subgroup. No obvious differences in biodistribution were noted between different subgroups by visual comparison.

Blood pool activity is only visible at 10 min after injection, with weak delineation of the heart and large blood vessels. Uptake is mainly seen in kidneys, liver and intestines. This uptake pattern is already present at the 10 min images and decreases over time. Weak uptake is seen in glandular tissues, such as thyroid, pituitary, salivary, lacrimal and sweat glands.

The uptake of ^{68}Ga-HER2-Nanobody in individual organs is presented in Figure 2 and Table S1. Blood pool activity is presented in Figure 3. A fast

blood clearance is seen, with only 10% of injected activity remaining in the blood at 1h p.i. Blood half-lives were calculated at 2.9 min (early phase) and 25.5 min (late phase). Plasma curves were identical to blood curves, indicating that the tracer was not associated to blood cells (data not shown). No metabolites were detected in blood up to 10 min or urine up to 2h p.i.

All images showed uptake in kidneys and excretion of the tracer into the urine. Although liver and intestinal uptake was visible, there were no signs of hepatobiliary excretion, such as accumulation in the gall bladder or duodenum. At 1h p.i., 50% of the tracer had been eliminated from the body, resulting in an estimated biological half-life of 1h (figure S2).

Effect of injected mass on liver uptake

Based on preclinical results, an effect of the injected mass of the compound on the non-specific binding was expected. Therefore, liver uptake was assessed in the three patient subgroups receiving different amounts of Nanobody mass. Overall, liver uptake was quite variable between patients. There is a trend towards lower liver uptake at 90 min p.i. or the 1.0 mg mass group, with an average uptake of 5.5 %IA compared to 9.0 and 9.5 %IA for 0.1 and 0.01 mg respectively, but with overlapping 95% confidence intervals (3.3-7.6; 5.7-12.3 and 7.4-11.5 respectively). A one-way ANOVA indicates no significant difference, $F(2,15) = 3.60$, $p = .053$.

Dosimetry

Table 2 summarizes the individual organ doses and individual effective dose (ED) results for all subjects with normal liver and renal function. The urinary

bladder wall shows the highest organ dose of 0.406 mGy/MBq, followed by the kidneys (0.216 mGy/MBq), liver (0.0778 mGy/MBq), lower large intestine wall (0.0759 mGy/MBq) and upper large intestine wall (0.0619 mGy/MBq).

Uptake in tumor lesions

Uptake in tumor lesions could be evaluated in 19 patients, 9 of which only had a primary lesion, six both a primary lesion and local or distant metastases, and 4 only local or distant metastases (Table 1).

Uptake in primary lesions

Tracer uptake was visible above background in 17 out 19 primary tumors, with SUV_{mean} values ranging between 0.7 and 11.8 (Table 1). Representative images showing ^{68}Ga-HER2-Nanobody uptake in primary lesions are presented in Figure 4.

Uptake in local and distant metastases

All patients with metastatic lesions showed clear tracer accumulation in at least one lesion, with SUV_{mean} ranging from 3.1 to 6.0. Figure 5 shows images of patients 18 and 20 with metastases in thoracic lymph nodes and the pelvis respectively. Supplementary movie S1 shows PET images of patient 14 with both a primary lesion and axillary lymph node metastasis.

Heterogeneous uptake pattern

In patient 8, a heterogeneous uptake pattern was observed in the primary tumor (Fig S3A). The uptake pattern did not match the FDG uptake pattern, indicating it was not caused by necrotic tumor areas. The patient presented

with diffuse metastases, of which some but not all lesions showed uptake above background (SUV_{mean} range 1.0-5.6; Fig S3B-C).

Discussion

This First-in-Human application of a radiolabeled Nanobody demonstrates the safety of the procedure with no observed adverse reactions related to the tracer administration. The ^{68}Ga-HER2-Nanobody tracer shows a favorable biodistribution, with the highest uptake in kidneys, liver and intestines, but very low background levels in all other organs that typically harbor primary breast carcinoma or tumor metastasis. ADA measurements showed that no pre-existing or tracer-induced antibodies against the Nanobody could be detected.

Rapid tracer clearance from the blood allows imaging at early time points (60 to 90 min p.i.) without the risk of false-positive signal due to blood pool activity. Tracer elimination occurs through the renal system, with high accumulation in the kidneys, similar to patterns described for other labeled peptides and small proteins (*17-19*) and as expected from Nanobody uptake patterns in rodents (*20*). Organs with substantial uptake are liver and intestines. Although a low expression of HER2 in liver is described in literature, the uptake most likely is of non-specific nature, given the high and probably supra-physiological uptake values (*21*). Liver uptake might obscure liver metastases, but given the absence of liver metastases in this patient group, the question remains unanswered. Based on preclinical observations, increasing amounts of protein up to 1 mg were administered in three different patient subgroups in an attempt to decrease non-specific binding, but no significant effect was observed.

Since liver uptake continues to decrease between the 60 and 90 min p.i., the latter is proposed as the best time point to obtain images with an optimal

signal-to-noise ratio. Later time points were not assessed in this study because of the short half-life of ^{68}Ga.

Whole body imaging revealed weak tracer uptake in glandular tissues such as salivary glands, pituitary, lacrimal glands and axillary sweat glands. This pattern was also observed with ^{68}Ga- and ^{111}In- labeled anti-HER2-affibody (*22*). The origin of this uptake remains to be determined, and might be related to low levels of HER2 expression or chelator-mediated trapping mechanisms. Clinical testing of ^{18}F-anti-HER2-Nanobody could provide more insight (*23*). It is however noteworthy that prostate-specific membrane antigen tracers show even more pronounced glandular uptake for both ^{68}Ga- and ^{18}F-labeled compounds, suggesting a specific uptake mechanism (*18,24*).

The urinary bladder wall received the highest organ dose of 0.406 mGy/MBq, which, at the highest injected activity of 185 MBq, is well below 100 mGy, thereby excluding potential deterministic effects. The average radiation burden was 0.04 mSv/MBq, which resulted in an average effective dose of 4.6 mSv for the 18 patients in this study. Maintaining a maximum activity of 185 MBq for future imaging studies, the highest effective dose would be 7.9 mSv. These values are acceptable for a diagnostic procedure and in line with other ^{68}Ga and ^{18}F PET radiotracers (*17,25*).

Although not the primary objective of this phase I study, tumor uptake values were evaluated in these breast carcinoma patients, both in primary lesions and metastases.

Uptake in primary lesions showed a wide uptake range between 0.7 and 11.8. This wide range could be due to the heterogeneous composition of primary lesions, with tumor cells infiltrating into normal breast tissue. Moreover patient no. 20 with SUV_{mean} of 0.7 had received 4 cycles of chemotherapy, which could explain the negative result. Additionally carcinoma *in situ* can coincide with infiltrating carcinoma, which can mimic the uptake in the invasive carcinoma, since these carcinoma *in situ* can also overexpress HER2, while not being correlated to the HER2 expression in metastatic lesions. ^{68}Ga-HER2-Nanobody PET/CT might therefore not be ideal for assessing HER2 expression in primary breast carcinoma lesions.

In metastatic patients however, a distinct uptake was seen in the majority of their metastases. In two of these patients, the tumor was classified as HER2-negative, based on IHC 2+ and FISH- results in the primary tumor. The increased tracer uptake might be related to intermediate HER2 expression (IHC 2+) or to discordance in HER2 expression between the primary lesion and the metastasis, as is described in literature in 14 to 30% of cases (*7,10*). Given the absence of direct histopathological correlation in this phase I study, a final conclusion cannot be made based on the current results. Sensitivity and specificity for the determination of HER2 status will be answered only through larger, prospective, and more clinically focused imaging trials.

Other research groups have in parallel developed PET/CT imaging strategies using the full antibody trastuzumab, used for therapy, labeled with ^{89}Zr or ^{64}Cu (*26,27*). This approach however has the disadvantage of slow blood clearance, resulting in a late imaging time point of 1-2 days (^{64}Cu) or 4-5 days (^{89}Zr) after tracer injection, a long scanning time up to 1h and a high radiation burden for

the patient of 12 (^{64}Cu) and 18 mSv (^{89}Zr) (*26,28,29*). To overcome these disadvantages, antibody fragments derived from trastuzumab, such as F(ab')$_2$ have been developed and labeled with shorter-lived isotopes. ^{68}Ga-DOTA-F(ab')$_2$-trastuzumab showed minimal or no tumor uptake in most cases, potentially related to suboptimal mass, lower immunoreactivity or a blood-half-life of the tracer that is too long to allow adequate PET-imaging with ^{68}Ga (*30*). Moreover, trastuzumab-derived tracers bind, contrary to ^{68}Ga-HER2-Nanobody, to the same epitope as the therapeutic agent, resulting in changes of uptake by differences in circulating therapeutic compound. The Affibodies labeled with ^{68}Ga and ^{111}In are also explored as tracers for HER2-imaging. The First-in-Human data have been published in 2010 (*22*). Meanwhile, a second compound against HER2 has been tested in a First-in-Human study, with a decrease in liver uptake (*19*). In total, 10 patients have been imaged with the different compounds, showing fast blood clearance and high potential for tumor targeting, similar to what is reported in this paper (*19,22*).

This First-in-Human use of radiolabeled Nanobody exemplifies the translational potential of a variety of preclinically tested Nanobody, raised against a multitude of targets such as Macrophage Mannose receptor (MMR) for assessment of the tumor microenvironment and Vascular Cell Adhesion Molecule 1 (VCAM1) in atherosclerosis (*31,32*). In combination with improvement of radiochemical techniques for ^{18}F-labeling, allowing distribution of tracers to multiple centers, this anti-HER2-Nanobody could just be the start of a number of exciting new PET-agents. Moreover, the recent developmental of targeted radionuclide therapy using ^{177}Lu-labeled anti-HER2-Nanobody

shows impressive preclinical results (*33*). Such a theranostic approach will be translated into a clinical trial in the near future.

Conclusion

^{68}Ga-HER2-Nanobody PET/CT is a safe procedure with a radiation dose comparable to other routinely used PET tracers. Its biodistribution is favorable, with the highest uptake in kidneys, liver and intestines, but very low background levels in all other organs that typically house primary breast carcinoma or tumor metastasis. Tracer accumulation in metastases of HER2 overexpressing patients is high, compared to normal surrounding tissues, and warrants further assessment in a phase II trial.

Disclosure

FPD received honoraria, was paid for consulting or has received travel and accommodation expenses from Roche, Teva, Novartis, Pfizer, Amgen; TL from Bayer-Schering, National Institute for Radioelements (IRE); MK from Biospacelab. TL and ND are co-founders of CamelIDs. TL has received funding from Boehringer-Ingelheim, Complix. MK, ND and TL have patents on Nanobody imaging and therapy.

Acknowledgments:

The authors thank Gratienne Van Holsbeeck and Martine Van den Broeck for their assistance in radiotracer preparations; the nurses Wendy Kemps, Nadine Eersels, Carl Van Halewijn, Annick Luppens, Claudia Housen, Magda Boels, Vanessa Quibus, Nathalie Blondeel and Françoise Henri for their assistance during the trial and their help in patient inclusion. MK and TL are Senior Clinical Investigators of the Research Foundation–Flanders (FWO). CV is supported by the GROUP-ID consortium of Ghent University. Research was funded by CancerPlan Action29 (Federal Public Service Health, Food Chain Safety and Environment, Belgium), Stichting tegen Kanker, FWO.

References

1. Slamon DJ, Leyland-Jones B, Shak S, et al. Use of chemotherapy plus a monoclonal antibody against HER2 for metastatic breast cancer that overexpresses HER2. *N Engl J Med.* 2001;344:783-792.

2. Hurvitz SA, Dirix L, Kocsis J, et al. Phase II randomized study of trastuzumab emtansine versus trastuzumab plus docetaxel in patients with human epidermal growth factor receptor 2-positive metastatic breast cancer. *J Clin Oncol.* 2013;31:1157-1163.

3. Kaufman PA, Bloom KJ, Burris H, et al. Assessing the discordance rate between local and central HER2 testing in women with locally determined HER2-negative breast cancer. *Cancer.* 2014;120:2657-2664.

4. Reddy JC, Reimann JD, Anderson SM, Klein PM. Concordance between central and local laboratory HER2 testing from a community-based clinical study. *Clin Breast Cancer.* 2006;7:153-157.

5. Fabi A, Di Benedetto A, Metro G, et al. HER2 protein and gene variation between primary and metastatic breast cancer: significance and impact on patient care. *Clin Cancer Res.* 2011;17:2055-2064.

6. Gancberg D, Di Leo A, Cardoso F, et al. Comparison of HER-2 status between primary breast cancer and corresponding distant metastatic sites. *Ann Oncol.* 2002;13:1036-1043.

7. Lower EE, Glass E, Blau R, Harman S. HER-2/neu expression in primary and metastatic breast cancer. *Breast Cancer Res Treat.* 2009;113:301-306.

8. Santinelli A, Pisa E, Stramazzotti D, Fabris G. HER-2 status discrepancy between primary breast cancer and metastatic sites. Impact on target therapy. *Int J Cancer.* 2008;122:999-1004.

9. Sapino A, Goia M, Recupero D, Marchio C. Current challenges for HER2 testing in diagnostic pathology: state of the art and controversial issues. *Front Oncol.* 2013;3:129.

10. Zidan J, Dashkovsky I, Stayerman C, Basher W, Cozacov C, Hadary A. Comparison of HER-2 overexpression in primary breast cancer and metastatic sites and its effect on biological targeting therapy of metastatic disease. *Br J Cancer.* 2005;93:552-556.

11. Cardoso F, Costa A, Norton L, et al. ESO-ESMO 2nd international consensus guidelines for advanced breast cancer (ABC2). *Breast.* 2014;23:489-502.

12. Gainkam LO, Keyaerts M, Caveliers V, et al. Correlation between epidermal growth factor receptor-specific nanobody uptake and tumor burden:

a tool for noninvasive monitoring of tumor response to therapy. *Mol Imaging Biol.* 2011;13:940-948.

13. Vaneycken I, D'Huyvetter M, Hernot S, et al. Immuno-imaging using nanobodies. *Curr Opin Biotechnol.* 2011;22:877-881.

14. Vaneycken I, Devoogdt N, Van Gassen N, et al. Preclinical screening of anti-HER2 nanobodies for molecular imaging of breast cancer. *FASEB J.* 2011;25:2433-2446.

15. Xavier C, Vaneycken I, D'Huyvetter M, et al. Synthesis, preclinical validation, dosimetry, and toxicity of 68Ga-NOTA-anti-HER2 Nanobodies for iPET imaging of HER2 receptor expression in cancer. *J Nucl Med.* 2013;54:776-784.

16. Stabin MG, Sparks RB, Crowe E. OLINDA/EXM: the second-generation personal computer software for internal dose assessment in nuclear medicine. *J Nucl Med.* 2005;46:1023-1027.

17. Sandstrom M, Velikyan I, Garske-Roman U, et al. Comparative biodistribution and radiation dosimetry of 68Ga-DOTATOC and 68Ga-DOTATATE in patients with neuroendocrine tumors. *J Nucl Med.* 2013;54:1755-1759.

18. Afshar-Oromieh A, Malcher A, Eder M, et al. PET imaging with a [68Ga]gallium-labelled PSMA ligand for the diagnosis of prostate cancer: biodistribution in humans and first evaluation of tumour lesions. *Eur J Nucl Med Mol Imaging.* 2013;40:486-495.

19. Sorensen J, Sandberg D, Sandstrom M, et al. First-in-human molecular imaging of HER2 expression in breast cancer metastases using the 111In-ABY-025 affibody molecule. *J Nucl Med.* 2014;55:730-735.

20. Gainkam LO, Caveliers V, Devoogdt N, et al. Localization, mechanism and reduction of renal retention of technetium-99m labeled epidermal growth factor receptor-specific nanobody in mice. *Contrast Media Mol Imaging.* 2011;6:85-92.

21. Cohen JA, Weiner DB, More KF, et al. Expression pattern of the neu (NGL) gene-encoded growth factor receptor protein (p185neu) in normal and transformed epithelial tissues of the digestive tract. *Oncogene.* 1989;4:81-88.

22. Baum RP, Prasad V, Muller D, et al. Molecular imaging of HER2-expressing malignant tumors in breast cancer patients using synthetic 111In- or 68Ga-labeled affibody molecules. *J Nucl Med.* 2010;51:892-897.

23. Vaneycken I, Xavier C, Blykers A, Devoogdt N, Caveliers V, Lahoutte T. Synthesis and first in vivo evaluation of 18F-anti-HER2-Nanobodies: a new probe for PET imaging of HER2 expression in breast cancer. Abstract 9. *J Nucl Med.* 2011;52:664.

24. Szabo Z, Mena E, Rowe SP, et al. Initial evaluation of [F]DCFPyL for prostate-specific membrane antigen (PSMA)-targeted PET imaging of prostate cancer. *Mol Imaging Biol.* 2015.

25. Mattsson S, Johansson L, Leide Svegborn S, et al. Radiation dose to patients from radiopharmaceuticals - Addendum 4 to ICRP publication 53. *ICRP Publication 106. Ann. ICRP 38 (1-2).* [http://www.icrp.org/docs/Radiation Dose to Patients from Radiopharmaceuticals - A fourth addendum to ICRP Publication 53.pdf. Accessed 20 May 2015.

26. Dijkers EC, Oude Munnink TH, Kosterink JG, et al. Biodistribution of 89Zr-trastuzumab and PET imaging of HER2-positive lesions in patients with metastatic breast cancer. *Clin Pharmacol Ther.* 2010;87:586-592.

27. Gebhart G, Lamberts LE, Garcia C, et al. PET/CT with 89Zr-trastuzumab and 18F-FDG to individualize treatment with trastuzumab emtansine (T-DM1) in metastatic HER2-positive breast cancer (mBC). *J Clin Oncol.* 2014;32: 695s suppl 15s:abstr 11001.

28. Keyaerts M, Xavier C, Heemskerk J, et al. First-in-human study of 68GaNOTA-Anti-HER2 Nanobody, a new radiopharmaceutical for Positron Emission Tomography (PET) Imaging of HER2 expression in breast carcinoma patients. *World Molecular Imaging Congress.* Vol Abstract ID 1990889 (SS 1). Seoul, South-Korea; 2014.

29. Mortimer JE, Bading JR, Colcher DM, et al. Functional imaging of human epidermal growth factor receptor 2-positive metastatic breast cancer using (64)Cu-DOTA-trastuzumab PET. *J Nucl Med.* 2014;55:23-29.

30. Beylergil V, Morris PG, Smith-Jones PM, et al. Pilot study of 68Ga-DOTA-F(ab')2-trastuzumab in patients with breast cancer. *Nucl Med Commun.* 2013;34:1157-1165.

31. Broisat A, Hernot S, Toczek J, et al. Nanobodies targeting mouse/human VCAM1 for the nuclear imaging of atherosclerotic lesions. *Circ Res.* 2012;110:927-937.

32. Movahedi K, Schoonooghe S, Laoui D, et al. Nanobody-based targeting of the macrophage mannose receptor for effective in vivo imaging of tumor-associated macrophages. *Cancer Res.* 2012;72:4165-4177.

33. D'Huyvetter M, Vincke C, Xavier C, et al. Targeted radionuclide therapy with A 177Lu-labeled anti-HER2 nanobody. *Theranostics.* 2014;4:708-720.

Figure legends

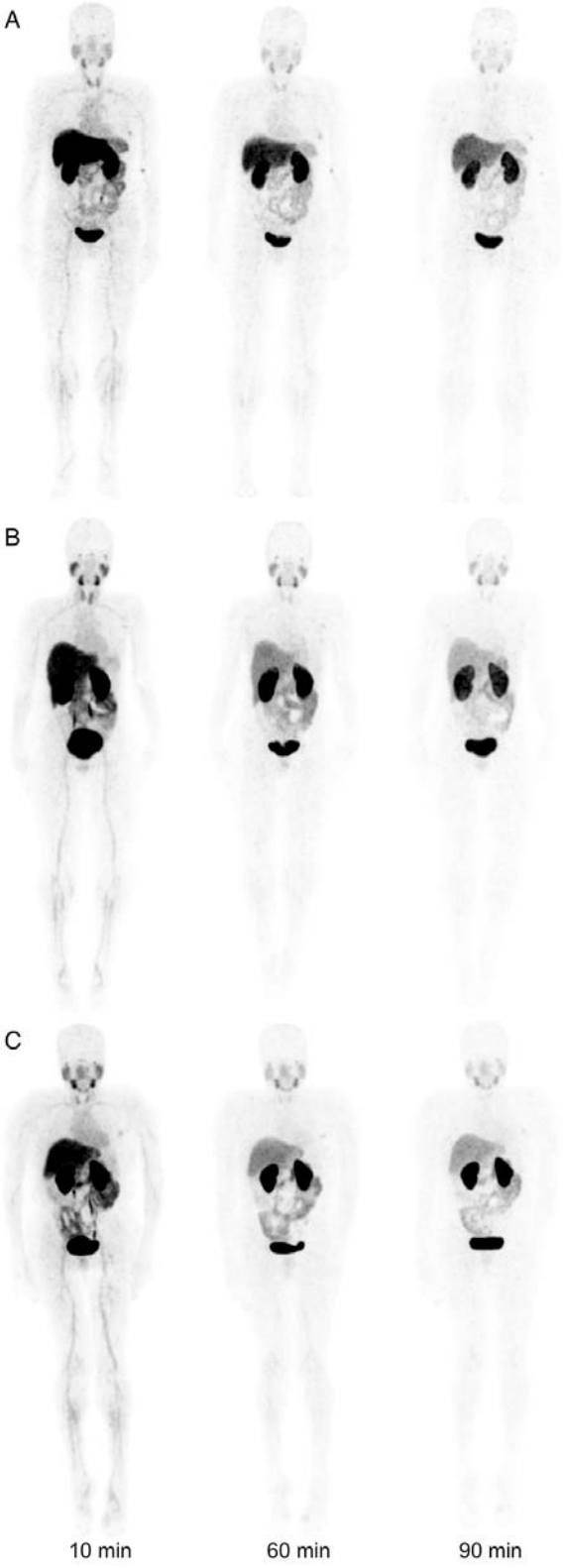

Figure 1. Representative maximum intensity projection (MIP) images at 10, 60 and 90 min p.i. of ^{68}Ga-HER2-Nanobody for the different mass subgroups. **A.** Patient 4, injected with 0.01 mg ^{68}Ga-HER2-Nanobody; **B.** Patient 12, injected with 0.1 mg ^{68}Ga-HER2-Nanobody; **C.** Patient 17, injected with 1.0 mg ^{68}Ga-HER2-Nanobody.

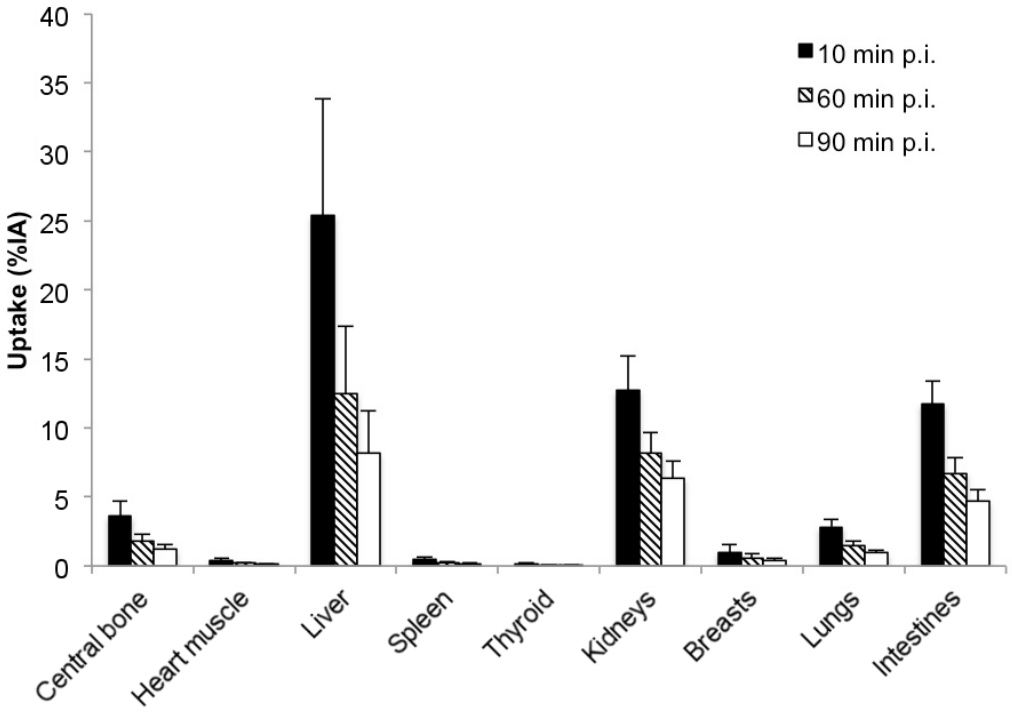

Figure 2. Uptake, expressed in % of injected activity (%IA) in different organs at 10, 60 and 90 min p.i. (n=18)

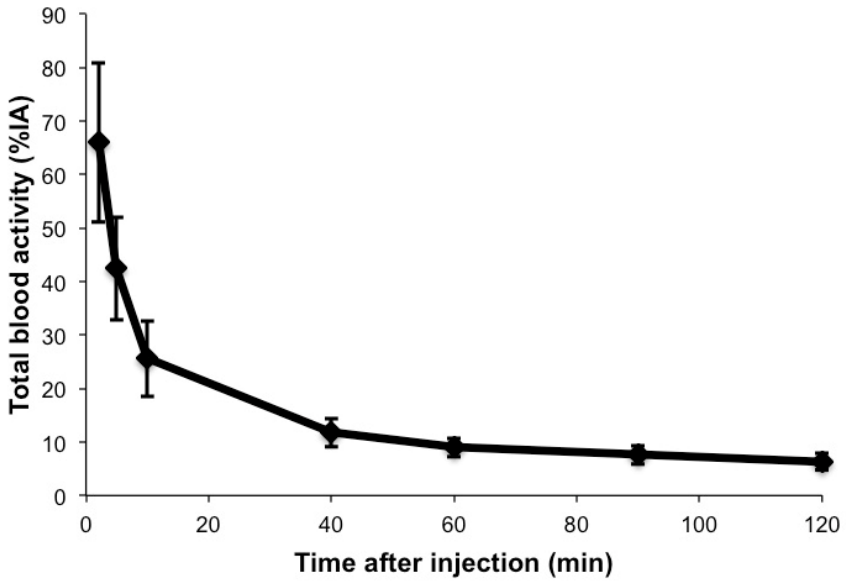

Figure 3. Time-activity curve of total blood activity, expressed in % of injected activity (%IA). Mean and standard deviation of 12 patients are represented.

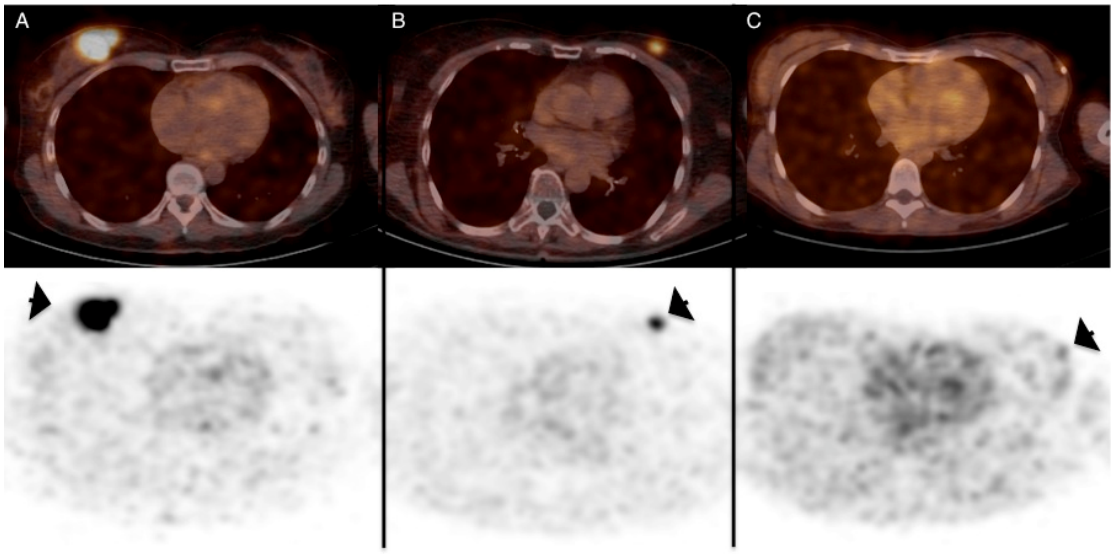

Figure 4. Uptake of ^{68}Ga-HER2-Nanobody in primary breast carcinoma lesions. This figure shows tracer uptake in primary lesions on fusion images (top row) and PET images (bottom row) with the lesion indicated by black arrows. **A**. Patient 14 showed the highest tracer uptake (SUV_{mean} 11.8). **B**. Patient 15 showed moderate tracer uptake, which is easily discernable from background (SUV_{mean} 4.9). **C.** Patient 6 showed no uptake in the primary lesion (SUV_{mean} 0.9); CT shows a marker clip at the tumor region.

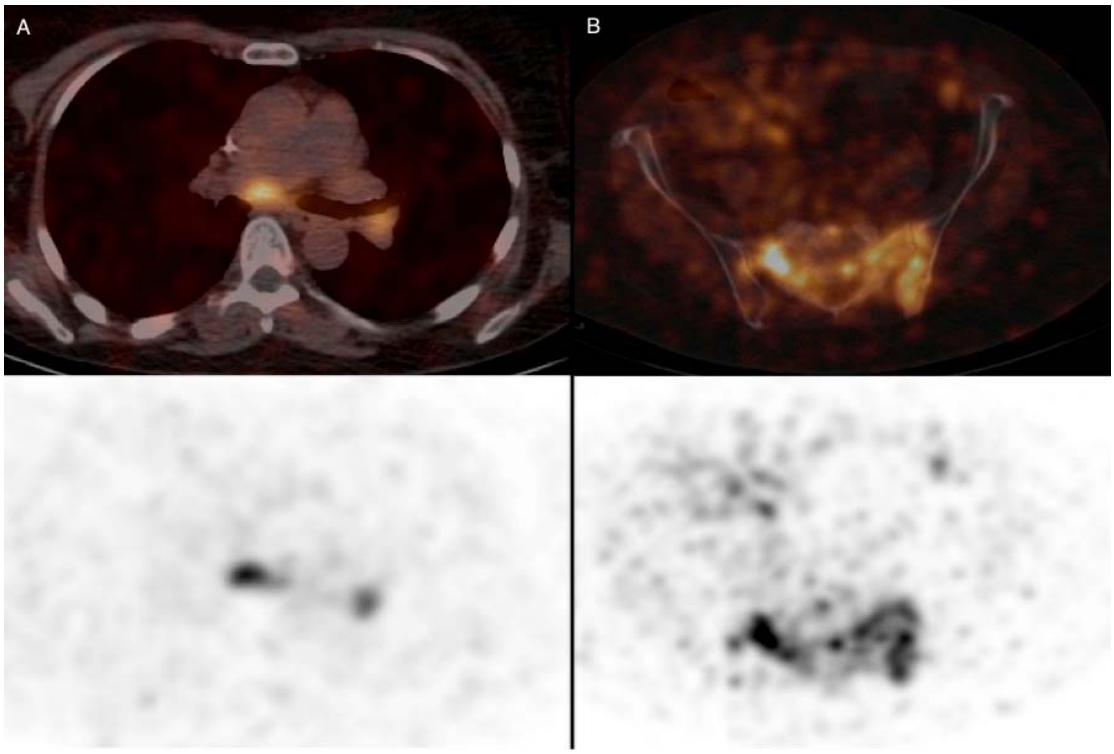

Figure 5. Uptake of ^{68}Ga-HER2-Nanobody in metastatic lesions on PET/CT fusion images (above) and PET images (below). **A.** Patient 18 with invaded lymph nodes in the mediastinum and left hilar region. **B.** Patient 20 with bone metastasis in the pelvis.

Table 1. Patient characteristics

	Patient no.	Age	Injected activity (MBq)	Tumor type	ER/PR	HER2 IHC	HER2 FISH (ratio; copies/cell)	Primary tumor	(Range of) SUV_{mean} of lesion(s) Local ADP	Distant M+ (type)
GROUP 1 0.01 mg	1	43	77	IDC	+/+	2+	+ (2.2; 6.2)	ISR*	A	A
	2	60	66	IDC	+/+	3+	+ (>2; macroclusters)	CR	A	3.1 (bone)
	3	68	53	IDC	+/+	3+	+ (12.2; 20.0)	3.2	A	A
	4	53	76	IDC	+/+	2+	- (1.3; 3.7)	2.2	A	A
	5	74	84	IDC	+/+	2+	- (1.3; 3.8)	2.3	A	A
	6	34	83	IMeC	+/-	3+	+ (2.8; 8.0)	0.9	A	A
	7	34	80	IDC	+/+	2+	- (1.0; 1.4)	2.0	A	A
GROUP 2 0.1 mg	8	67	92	IDC	+/+	2+	- (1.4; 3.4)	5.0	3.2-4.3	1.0-5.6 (bone)
	9	57	111	IDC	+/+	3+	+ (1.3; 6.1)	2.3	A	A
	10	61	100	IDC	+/-	3+	+ (9.4; 15.0)	SR	SR	4.1-5.7 (bone)
	11	65	90	IDC	+/+	3+	+ (2.3; 5.1)	2.9	6.3	A
	12	46	82	IDC	+/+	3+	+ (8.1; 15.6)	1.4	A	A
	13	32	153	IDC	-/-	2+	+ (9.4; 17.4)	3.2	1.7	A
	14	53	103	IDC	-/-	3+	+ (4.7; 9.2)	11.8	13.0	A
	15	78	148	IDC	+/+	2+	- (1.0; 2.1)	4.9	A	A
GROUP 3 1.0 mg	16	76	96	ILC	+/+	2+	- (1.0; 1.7)	SR	SR	2.2-3.9 (bone)
	17	74	138	IDC	-/-	2+	- (1.2; 4.3)	1.8	A	A
	18	62	167	IDC	+/-	2+	+ (2.6; 4.5)	SR	SR	3.5-6.0 (ADP mediastinum)
	19	62	174	IMiC	+/+	3+	+ (2.8; 8.0)	4.4	5.1-5.9	3.6-3.9 (bone)
	20	48	170	IDC	+/+	3+	+ (7.8; 15.6)	0.7†	A	4.7-5.4 (bone)†

*IDC = invasive ductal carcinoma; ILC = Invasive lobular carcinoma; ER = estrogen receptor; PR = progesterone receptor; IMeC = Invasive medullary carcinoma; IMiC = Invasive Mixed carcinoma; ADP = adenopathy; ISR = incomplete surgical removement; CR = complete response on CT; SR = surgically removed; A = Absent; * = patient was scanned after incomplete surgical removement but additional surgical resection could not demonstrate remaining tumor cells; † = after 4 cycles of epirubicine-cyclophosphamide;*

Table 2. Organ doses and effective dose

Patient no.	Organ dose (mGy/MBq)						Effective dose (mSv/MBq)
	Urinary Bladder Wall	Kidneys	Liver	LLI Wall	ULI Wall	Thyroid	
1	0.406	0.191	0.0515	0.0843	0.0606	0.0233	0.0425
3	0.406	0.161	0.114	0.0757	0.0679	0.0326	0.0458
4	0.405	0.219	0.0788	0.0295	0.0787	0.0257	0.0371
5	0.407	0.181	0.116	0.0962	0.0566	0.0093	0.0472
6	0.406	0.297	0.0957	0.0798	0.0535	0.0282	0.0453
7	0.405	0.259	0.0788	0.0423	0.0840	0.0020	0.0371
8	0.405	0.141	0.114	0.0788	0.0715	0.0137	0.0433
9	0.406	0.273	0.0740	0.0686	0.0675	0.0200	0.0421
10	0.406	0.229	0.0922	0.0626	0.0991	0.0035	0.0425
12	0.407	0.220	0.0594	0.0816	0.0772	0.0327	0.0435
13	0.406	0.225	0.113	0.0632	0.0812	0.0496	0.0442
14	0.407	0.222	0.0849	0.0719	0.113	0.0513	0.0448
15	0.406	0.278	0.0719	0.0086	0.0071	0.0035	0.0335
16	0.407	0.192	0.0473	0.140	0.0356	0.0124	0.0485
17	0.407	0.216	0.0610	0.141	0.0518	0.0132	0.0504
18	0.406	0.193	0.0583	0.118	0.0554	0.0110	0.0469
19	0.406	0.181	0.0422	0.0087	0.0067	0.0220	0.0317
20	0.406	0.211	0.0469	0.116	0.0464	0.0177	0.0447
Mean ± SD	0.406±0.001	0.216±0.041	0.0778±0.0252	0.0759±0.0384	0.0619±0.0274	0.0207±0.0143	0.0428±0.0050

Patient no. 2 and 11 were not taken into account because of altered liver and/or kidney function.
LLI = Lower large intestines; ULI = Upper large intestines.